

# Attribution of River-Sourced Floating Plastic in the South Atlantic Ocean Using Bayesian Inference

Claudio Pierard<sup>1</sup>, Deborah Bassotto<sup>1</sup>, Florian Meirer<sup>2</sup>, Erik van Sebille<sup>1</sup>

<sup>1</sup>Utrecht University, Institute for Marine and Atmospheric Research, Princetonplein 5, 3584 CC Utrecht, Netherlands

<sup>2</sup>Utrecht University, Debye Institute for Nanomaterials Science, Inorganic Chemistry and Catalysis, Universiteitsweg 99, 3584 CG Utrecht, Netherlands

## Key Points:

- We developed a probabilistic framework to attribute the sources of floating oceanic plastic
- The framework uses Bayes theorem to combine river plastic emissions with Lagrangian simulations
- The framework yields probability maps and age distributions of the most likely source in the region

---

Corresponding author: Claudio Pierard, [c.m.pierard@uu.nl](mailto:c.m.pierard@uu.nl)

## 15 **Abstract**

16 Most marine plastic pollution originates on land. However, once plastic is at sea, it is  
 17 difficult to determine its origin. Here we present a Bayesian inference framework to com-  
 18 pute the probability that a piece of plastic found at sea came from a particular source.  
 19 This framework combines information about plastic emitted by rivers with a Lagrangian  
 20 simulation, and yields maps indicating the probability that a particle sampled somewhere  
 21 in the ocean originates from a particular source. We applied the framework to the South  
 22 Atlantic Ocean, focusing on floating river-sourced plastic. We computed the probabil-  
 23 ity as a function of the particle age, at three locations, showing how probabilities vary  
 24 according to the location and age. We computed the source probability of beached par-  
 25 ticles, showing that plastic found at a given latitude is most likely to come from the clos-  
 26 est source. This framework lays the basis for source attribution of marine plastic.

## 27 **Plain Language Summary**

28 Plastic is commonly found floating near the surface of the ocean but it is difficult  
 29 to know where it was introduced into the environment. For some large plastic items, the  
 30 origin can be estimated by analysing the information printed on them, but for small par-  
 31 ticles, this information is typically missing. To estimate the origin of particles at sea, we  
 32 built a framework that assigns a probability indicating the chance of finding a particle  
 33 that came from a particular source, found at a specific location of the ocean. The frame-  
 34 work uses estimates of plastic emitted by rivers, in combination with a simulation of the  
 35 transport of particles at the ocean surface, to compute the probability that a particle,  
 36 found at a particular location in the South Atlantic, comes from a certain river. Sim-  
 37 ilarly, we computed the probability that a particle of a certain age (defined as the time  
 38 it has been drifting in the ocean) comes from a particular river, showing that the prob-  
 39 ability changes according to the particle age. Finally, we computed the probability for  
 40 particles stranded at the coasts of South America and Africa, showing that plastic found  
 41 on beaches is most likely to come from the closest river.

## 42 **1 Introduction**

43 Floating plastic items have been found in all of the world’s oceans (Eriksen et al.,  
 44 2014; Van Sebille et al., 2015), but the origins (i.e. where and when the plastic entered  
 45 the ocean) of these plastic items are often not obvious. For some of the larger macroplas-  
 46 tics, the origin can be attributed by careful analysis of labels (e.g. Lebreton et al. (2018);  
 47 Schofield et al. (2020); Turner et al. (2021)), but most (micro)plastic particles are too  
 48 small and nondescript for their origin to be identified this way. Nevertheless, it is im-  
 49 portant to assess and possibly attribute the likely source for these smaller particles too,  
 50 as they are among the most harmful to marine ecosystems (Koelmans et al., 2019).

51 Here, we use numerical simulations to compute the pathways of virtual plastic par-  
 52 ticles that float on the surface of the ocean (Hardesty et al., 2017; Van Sebille et al., 2018).  
 53 By tracking particles, it is in principle possible to connect any source with any location.  
 54 However, the multitude of possible sources very quickly makes this a computationally  
 55 unwieldy approach. To overcome this computational challenge, we here propose using  
 56 a Bayesian inference approach to attribute sources in a probabilistic sense.

57 Such a probabilistic approach has been used before to locate objects lost at sea,  
 58 like the submarine *Scorpio* (Richardson et al., 1971) and the (yet to be found) Malaysian  
 59 Airlines flight MH370 (Davey et al., 2016). The main difference between these search &  
 60 rescue applications of Bayesian inference and our application in the source attribution  
 61 of floating plastic is that the sources of plastic are spatially very heterogeneous, and so  
 62 is its distribution at sea.

To develop this probabilistic framework for attribution of likely plastic sources, we here focus on plastic emitted by rivers, as rivers are considered the principal pathway for mismanaged plastic waste (MPW) into the ocean (Lebreton & Andrady, 2019). We selected the South Atlantic Ocean as the study location because the South Atlantic Sub-tropical Gyre is an accumulation zone for plastic (Cózar et al., 2014; Ryan, 2014; Morris, 1980), but also because of the presence of large urban centers along the American and African coast that contribute to the plastic found at sea (Jambeck et al., 2018; do Sul & Costa, 2007), and because we plan to compare our results with samples collected during a 2019 expedition to the region.

## 2 Theory

Bayesian inference uses Bayes' Theorem to estimate the conditional probability of an event happening under certain conditions by combining prior knowledge about the problem with data obtained through an experiment. In particular, our objective is to estimate the probability that a particle sampled at sea would come from a certain source. This can be written as the conditional probability  $p(R_i|S_{loc})$ : the probability of sampling a particle at a location  $S_{loc}$  from a specific source  $R_i$ .

Bayes' theorem offers a way of estimating  $p(R_i|S_{loc})$ , by combining prior knowledge with new observations. In our case, Bayes' theorem is

$$p(R_i|S_{loc}) = \frac{p(S_{loc}|R_i)p(R_i)}{p(S_{loc})}, \quad (1)$$

where  $p(R_i|S_{loc})$  is the conditional probability that we aim to estimate,  $p(S_{loc}|R_i)$  is the opposite conditional probability that can be estimated by performing a numerical simulation (see below),  $p(R_i)$  is the probability of a particle being released at a particular source and  $p(S_{loc})$  is the probability of sampling a plastic particle in a specific location, regardless of the source. It is important to note that  $p(R_i|S_{loc}) \neq p(S_{loc}|R_i)$ . The latter term namely indicates the probability of a plastic particle found at a location to come from a specific source, and the former indicates the probability of a particle coming from a specific source being at a location. Each term is commonly referred to by its interpretation. For instance,  $p(R_i)$  is denoted as 'the prior' because it represents the prior knowledge of the problem,  $p(S_{loc}|R_i)$  is 'the likelihood', which updates our prior knowledge from the problem,  $p(S_{loc})$  is the 'normalizing constant', and  $p(R_i|S_{loc})$  is 'the posterior'.

In eq. (1), computing the normalizing constant  $p(S_{loc})$  requires observations for all plastics in the ocean regardless of their source, which means that  $p(S_{loc})$  also considers plastic that comes from sources that are not taken into account in the numerator of eq. (1). Therefore, the posterior probabilities at each  $S_{loc}$  would not add to one in each location but instead will add to a fraction that corresponds only to the sources of plastic considered in the study. This is inconvenient when the focus is only on plastic coming from specific sources such as riverine plastic. To overcome this inconvenience, we can constrain the sum of all posterior probabilities to be equal to one

$$\sum_{i=1}^N p(R_i|S_{loc}) = 1, \quad (2)$$

where the sum is defined for the  $N$  number of sources. Then, substituting  $p(R_i|S_{loc})$  for eq. (1)

$$\sum_{i=1}^N \frac{p(S_{loc}|R_i)p(R_i)}{p(S_{loc})} = 1, \quad (3)$$

103 and by factorizing and solving for  $p(S_{loc})$

$$p(S_{loc}) = \sum_{i=1}^N p(S_{loc}|R_i)p(R_i), \quad (4)$$

104 we obtain a normalizing constant that only considers the sum of all our hypotheses (i.e.  
105 products of prior and likelihoods). Finally, by substituting  $p(S_{loc})$  in eq. (1) we get

$$p(R_i|S_{loc}) = \frac{p(S_{loc}|R_i)p(R_i)}{\sum_{i=1}^N p(S_{loc}|R_i)p(R_i)}, \quad (5)$$

106 which is an alternative form of Bayes' theorem (Carlin & Louis, 2008) that ensures that  
107 the sum of all posterior probabilities is one in each location. This last equation is used  
108 in this study.

### 109 3 Methodology

#### 110 3.1 Selecting the Sources and Computing the Prior

111 Our prior is based on the annual amount of riverine plastic estimated by Meijer  
112 et al. (2021), who used a probability framework combined with geographical data of MPW  
113 to estimate the plastic mass emissions of the world rivers into the ocean, at the location  
114 of the river mouths. From their global data set, we selected the locations and annual emis-  
115 sions for all 1,010 rivers that emit plastic into the South Atlantic. To avoid immediate  
116 beaching, we moved the river mouth locations to the center of the closest ocean grid-cell  
117 of the model's flow field. When various rivers shared the same closest grid-cell, we summed  
118 their emissions. This condensed the number of release locations to 535 (without affect-  
119 ing the total amount of plastic released by the rivers in the South Atlantic).

120 We then clustered the rivers in 10 groups that contained the top polluting rivers  
121 and their neighboring rivers. These clusters are 2° by 2° square regions centered around  
122 ten locations that coincide with important cities or river estuaries. We used the result-  
123 ing 283 river mouth locations in these 10 clusters as the release positions for the partic-  
124 les in the simulation. The 10 clusters (Figure 1) account for 87.9% of the riverine plas-  
125 tic emissions in the South Atlantic. There are two clusters on the African coast: around  
126 the city of Cape Town and on the Congo River estuary. The other eight clusters are on  
127 the South American coast: five near the cities of Rio de Janeiro, Porto Alegre, Santos,  
128 Salvador, and Recife; and three on the river estuaries of Rio de la Plata, Itajaí and Paraíba.

129 We defined the prior distribution  $p(R_i)$  to be the fraction of plastic emitted at each  
130 cluster, normalised by the total amount of plastic emitted at the 10 clusters. Our prior  
131 thus is a 10-dimensional categorical or discrete distribution, in which each source has an  
132 associated probability defined between 0 to 1, and the sum of the 10 probabilities is 1.  
133 The probability associated with each source is shown in Table S1.

#### 134 3.2 Simulation Setup and Computing the Likelihood

135 To compute the likelihood  $p(S_{loc}|R_i)$ , we released virtual particles from each of the  
136 sources  $R_i$  and tracked them through the South Atlantic surface flow. We performed the  
137 simulation using the Parcels framework (Delandmeter & Sebille, 2019) on the Surface  
138 and Merged Ocean Currents (SMOC) data set from the Copernicus Marine Environmen-  
139 tal Service (CMEMS) (Drillet et al., 2019). The SMOC data set is a 2D surface flow field,  
140 with a 1/12° resolution, of the sum of the velocity contributions from the Eulerian compo-  
141 nent associated with currents, the tidal component, and the Stokes Drift component  
142 associated with waves (Drillet et al., 2019). In this study we assumed that the particles  
143 were at the surface at all times.



**Figure 1.** Map of the top 50 rivers (red dots) in the South Atlantic from Meijer et al. (2021) and the clusters (black squares) used as sources in this study. The size of the red circles is proportional to the rivers' plastic emission. The size of the black squares exaggerates the true size of the clusters, which is  $2^\circ$  by  $2^\circ$ .

144 The domain of the simulation was the South Atlantic Ocean, from  $70^\circ\text{W}$  to  $25^\circ\text{E}$   
 145 and between  $50^\circ\text{S}$  to the Equator. We used hydrodynamic data from 1 April 2016 to 31  
 146 August 2020, releasing particles in the first year only and then tracking them for another  
 147 3.4 years. During the simulation, if a particle left the domain, we stopped tracking that  
 148 specific particle. We implemented a stochastic parametrization for beaching of buoyant  
 149 particles as described in Onink et al. (2021), using a beaching timescale of  $\lambda_b = 10$  days  
 150 and a re-suspension timescale of  $\lambda_r = 69$  days. To parametrise unresolved turbulence  
 151 that acts on the floating plastic (Van Sebille et al., 2020), we implemented uniform dif-  
 152 fusion defined in the whole domain with a value of  $10\text{ m}^2\text{ s}^{-1}$ , similar to Onink et al. (2021)  
 153 and Lacerda et al. (2019).

154 We performed one simulation with 100,000 particles per source, with a fourth-order  
 155 Runge-Kutta integration time step of 1 h. We released the particles from the 283 river  
 156 mouth locations inside the 10 clusters. On average, the particles were released 10 km from  
 157 the coast. The number of particles released at each location was proportional to the emis-  
 158 sion of each of the rivers within the cluster, and equally distributed over one year. We  
 159 stored the particles' positions every 24 h, for a total of 1,234 points per trajectory.

160 We computed the likelihood  $p(S_{loc}|R_i)$  by binning the particle positions in  $1^\circ \times 1^\circ$   
 161 bins. For this, we counted the particles inside each bin at every time step, and then we  
 162 averaged the number of particles during a time period. Then, we divided the average num-  
 163 ber of particles at each bin by the sum of all the averaged counts in all bins. The  $p(S_{loc}|R_i)$   
 164 in each bin has a value between 0 and 1 and the sum of the probabilities of all bins is  
 165 1. This yielded 10  $p(S_{loc}|R_i)$  maps, one per source  $R_i$ .

166 The likelihood was computed based on the positions of the particles according to  
 167 their age. The particle age represents the transit time of particles between the source  
 168  $R_i$  and a sampling location  $S_{loc}$  (i.e., their drifting time), with each particle following  
 169 a different pathway until reaching  $S_{loc}$  (Van Sebille et al., 2018). The likelihood results  
 170 are shown in Figure S1 and Text S1 of the supplementary material.

### 171 3.3 Oceanic Particles Posterior Probability

172 We computed the posterior probability  $p(R_i|S_{loc})$  using eq. (5) independently for  
 173 each  $1^\circ$  by  $1^\circ$  bin, using the corresponding likelihood and the normalizing constant in each  
 174 particular bin. Doing this for all the sources, we get the local posterior distribution in  
 175 each bin, as a probability between 0 and 1 for each source. This results in 10 posterior  
 176 probability maps (one per source) which add up to 1 for each bin.

### 177 3.4 Beached Particles Posterior Probability

178 Since we use a stochastic parametrization for simulating the beaching of particles  
 179 near the coast, we can also map the probability of a beached particle coming from a spe-  
 180 cific source. To compute this, we built two cumulative latitudinal histograms of the par-  
 181 ticles that were beached at a specific time step: one for the American coast and the other  
 182 for the African coast. The cumulative latitudinal histogram is formed by counting the  
 183 particles that are beached in latitudinal bins of  $1^\circ$ , disregarding the longitude of those  
 184 particles, and by classifying them into particles that beached either at the American or  
 185 the African coast. With the counts per latitude, we computed the average at each bin  
 186 for the duration of the whole simulation and normalized by the sum of all average counts  
 187 per bin. As for the posterior probability maps, we computed the beached posterior prob-  
 188 ability  $p(R_i|S_{lat})$  using eq. (5), where  $S_{lat}$  is the latitudinal bin.

## 189 4 Results

190 Figure 2 shows the posterior probability  $p(R_i|S_{loc})$  maps for each source, averaged  
 191 over 3.4 years. In particular, the particles in our simulation did not reach latitudes south  
 192 of  $50^\circ\text{S}$ , leading to no defined posterior probability in the Antarctic Circumpolar Cur-  
 193 rent (ACC). This is due to the generally northward Ekman drift in the ACC (Onink et  
 194 al., 2019), and because we assumed that the particles only originate from ten sources placed  
 195 north of  $50^\circ\text{S}$ . In total, 130,585 particles exited the domain: 97,926 across the Equator  
 196 and 32,659 into the Indian Ocean.

197 Regarding the individual panels in Figure 2, the posterior probabilities for Recife  
 198 and Santos were near-zero because only very few particles were transported into the open  
 199 ocean. The probability that particles that end up between  $50^\circ\text{W}$  to  $40^\circ\text{W}$  and close to  
 200 Brazil originated from Salvador was up to 30%. The posterior probabilities of Itajaí and  
 201 Paraíba were below 20% everywhere, with the highest values located in the subtropical  
 202 gyre, while probabilities were close to zero in the rest of the domain. For Rio de la Plata,  
 203 the highest probabilities were found at the boundary with the ACC, approaching 40%  
 204 in probability, with decreasing values when going from there towards the equator. The  
 205 two sources that dominated in the region of the subtropical gyre, between  $20^\circ\text{S}$  to  $50^\circ\text{S}$ ,  
 206 were Porto Alegre and Rio de Janeiro, with probabilities around 40%. South of South  
 207 Africa, particles released from Rio de Janeiro are dominant, contributing 60% to the prob-  
 208 ability. The remaining 40% are mainly contributed by Porto Alegre and Rio de la Plata.  
 209 In the Benguela Current region and extending northwest to the northern coast of Brazil,  
 210 the probability is close to 100% that particles originate from Cape Town. Finally, the  
 211 posterior probability of Congo is almost only located near the source and farther north.

### 212 4.1 Local Posterior Age Distributions

213 The posterior age distributions yield the probable sources of a particle of a certain  
 214 age, sampled at a certain location. Figure 3 shows the posterior age distributions for three  
 215 sampling locations, averaged over a time window of 30 days. The dashed line represents  
 216 the number ( $N$ ) of particles that reach the location as a function of age. The posterior  
 217 probability distributions were only computed when  $N > 10$ .

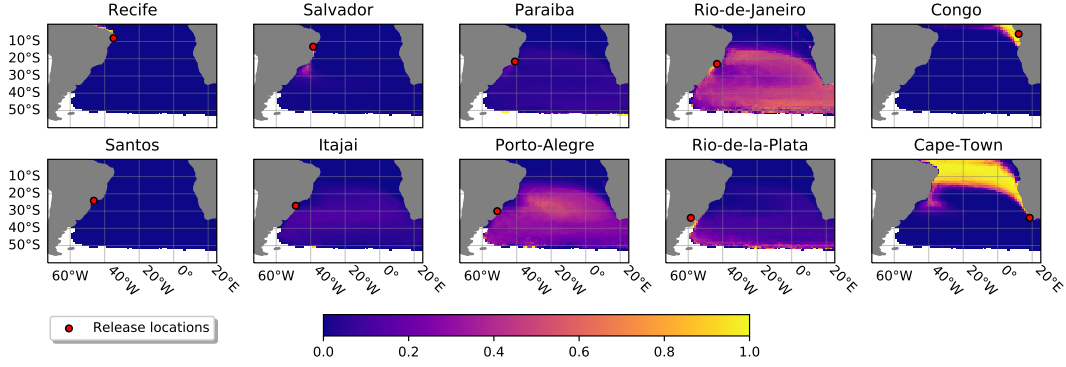


**Figure 2.** Posterior probability maps, averaged over 3.4 years, showing  $p(R_i|S_{loc})$ , the probability of finding a particle from a specific source at any point in the South Atlantic. Each map displays the probability for a specific source in all the bins of the domain. The red dots indicate the locations of the sources from which the particles entered the ocean.

218 The panel for sampling location A in Figure 3, located in the western part of the  
 219 subtropical gyre (32.37°S, 37.64°W), shows for example that a particle sampled at that  
 220 location with age younger than 0.4 years is very unlikely to come from any of the con-  
 221 sidered river sources. For particles between 0.4 years to 1.0 years, the most probable sources  
 222 are Salvador and Porto Alegre. For ages older than 1.0 years, the probability from Sal-  
 223 vador drops below 20% while Rio de Janeiro grows. For particles older than 1.5 years,  
 224 Porto Alegre and Rio de Janeiro have the largest probabilities, with values fluctuating  
 225 between 20% and 40%. The rest of the sources have values below 20%.

226 The posterior age distributions for location B (32.37°S, 5.80°E) in Figure 3, show  
 227 that it is unlikely to find particles younger than 1.2 years coming from any of the con-  
 228 sidered sources: only particles older than 1.4 years can reach this point. Similar to point  
 229 A, the sources with the largest probability, throughout all ages, are Rio de Janeiro and  
 230 Porto Alegre. For the younger particles, these probabilities oscillate around 50%, while  
 231 for older particles, the two sources decrease down to 30% for 3.4-year-old particles. The  
 232 remaining sources stay below 20% for all ages. The plot corresponding to point C located  
 233 north of the gyre (19.19°S, 13.39°W), shows that particles reach this location two years  
 234 after release. Fewer particles were present on average compared to A and B, reaching  
 235 a peak  $N$  at 2.7 years. The largest probability corresponds to Rio de Janeiro and Porto  
 236 Alegre. Rio de Janeiro is the predominant source of particles of all ages, although, Porto  
 237 Alegre becomes significant when particles are 2.5 years old or older. The other sources  
 238 remain below 10% for all ages recorded.

## 239 4.2 Beached Particles Posterior

240 Figure 4 shows the posterior probabilities for a particle to beach at certain latitude,  
 241  $p(R_i|S_{lat})$ , based on its origin. The  $p(R_i|S_{lat})$  for the American coast are displayed in  
 242 the right panel and the ones for the African coast are shown in the left panel. On the  
 243 American coast, the nearest source to the bin  $S_{lat}$  has the highest probability, which peaks  
 244 at the same latitude as the source or in its vicinity. This suggests that the plastic found  
 245 on beaches close to a source is most likely to come from that source. Santos is the only  
 246 exception to this trend because its probability is overshadowed by its proximity to Rio  
 247 de Janeiro which emissions are six times larger.

248 In the right panel of Figure 4, the beached probabilities for latitudes between 25°S  
 249 to 35°S on the African coastline show a dominance of particles coming from the Amer-

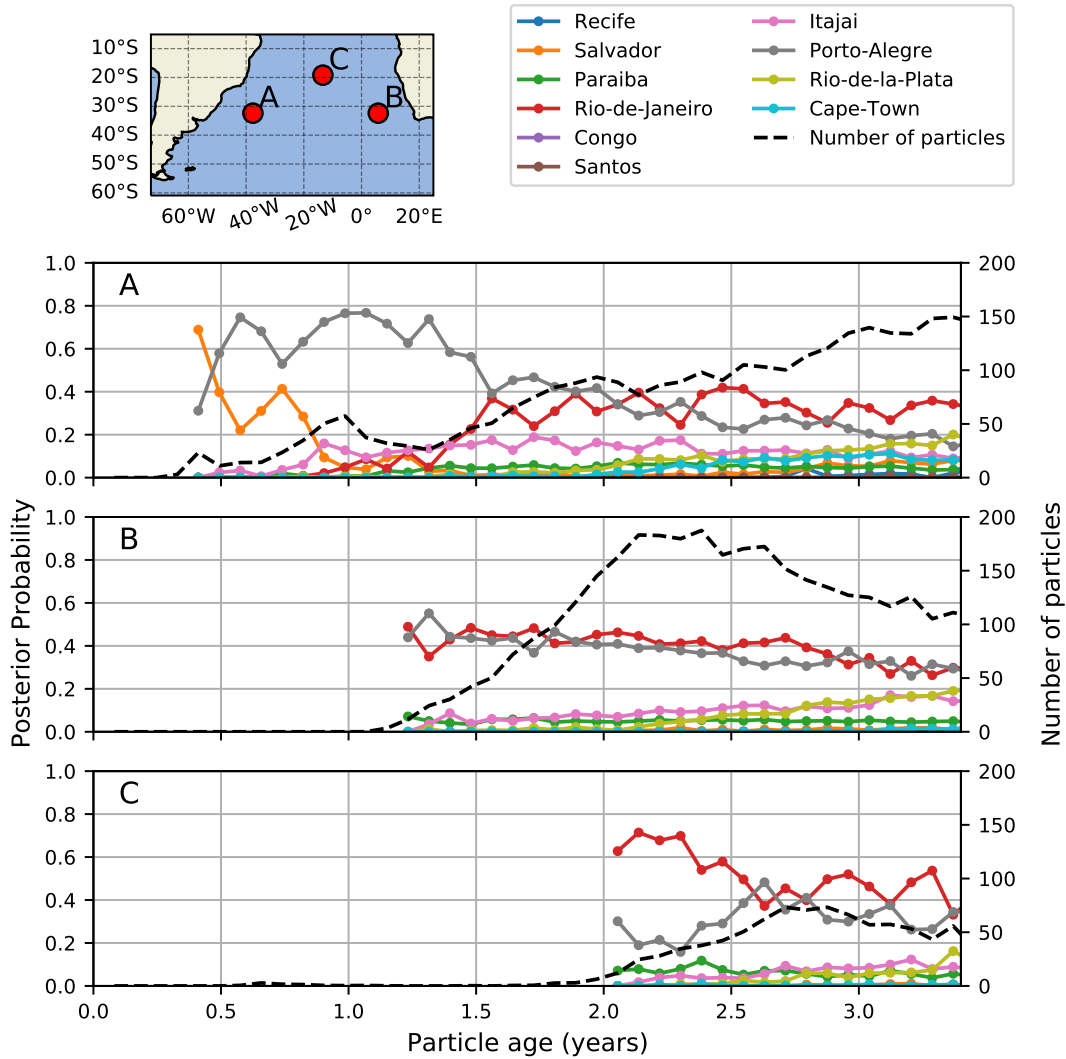


**Figure 3.** Local posterior age distributions at three different locations for the posterior probability. The map on the top right marks the locations A, B, and C, that correspond to the time series shown in the plots A, B, and C. Each color in A, B and C, represents the probability  $p(R_i|S_{loc})$  for a particular source. The black dashed line represents the number of particles ( $N$ ) at the respective location.

250 ican coast, accounting for 90% of the beached particles. The probability of the beached  
 251 particles coming from Cape Town was found to be less than 10% in this region. Between  
 252 18°S to 25°S, Cape town was the only source for beached particles. There were also re-  
 253 gions, namely between 12°S to 14°S and 16°S to 18°S, where no particles of any of the  
 254 considered sources beached. Finally, at latitudes between 5°S to 12°S, the only proba-  
 255 ble source was Congo, no particles from other sources beached that far north. The rea-  
 256 son that we found 100% probability for one single source or no beached particles at all,  
 257 is that we only considered two sources in Africa, which were at the borders of the stud-  
 258 ied domain. In the future, more sources need to be considered, both in this region and  
 259 outside, to improve these estimates.

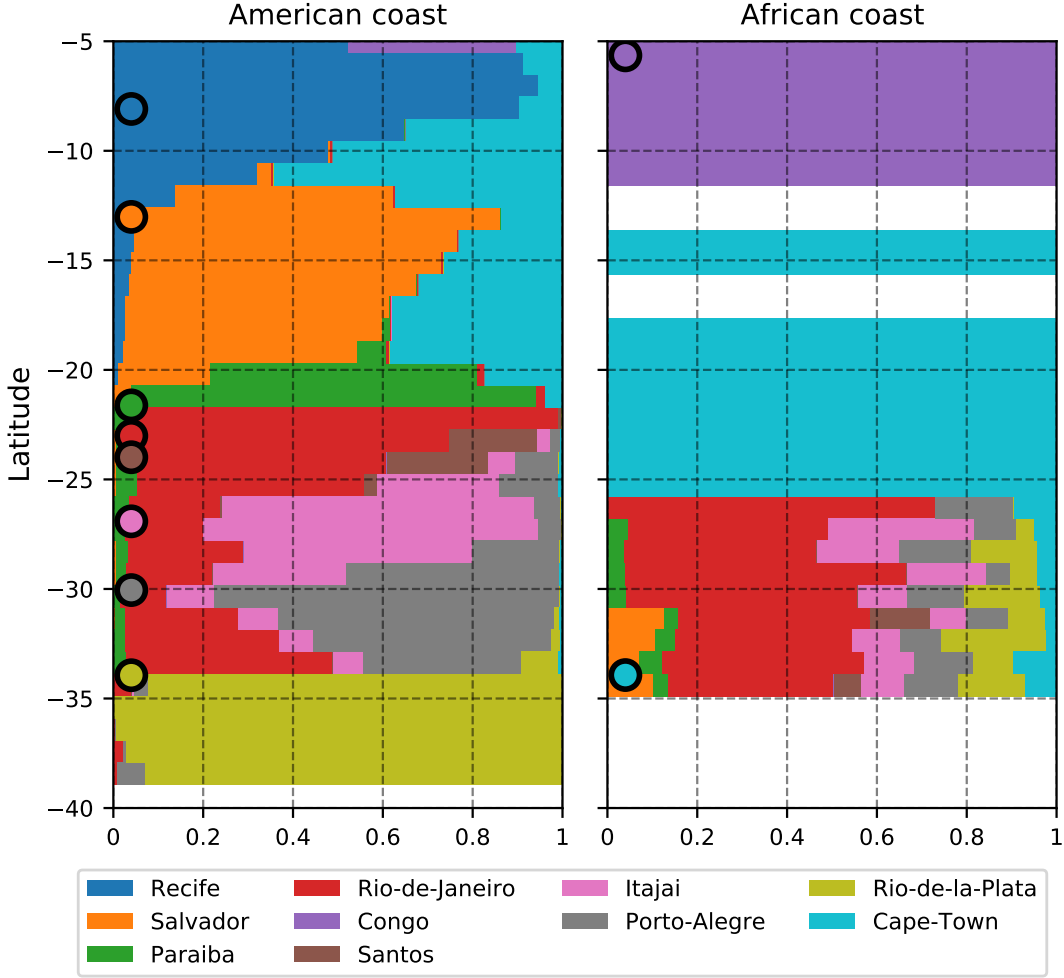


**Figure 4.** Horizontal bar plot for the posterior probabilities of beached particles ( $x$ -axis) at a specific latitude ( $y$ -axis). The panel on the left shows the probabilities at the American Coast and the panel on the right the probabilities at the African coasts. Each color is associated with a source, shown in the legend at the bottom. Each latitude has a corresponding horizontal bar summing the probabilities from the sources at that latitude to 1. The round markers on the left of each plot represent the latitudes of the sources. If the marker is on the left panel, the source is at the American coast, and if the marker is in the right panel, the source is located at the African coast.

## 5 Conclusions and Discussion

We introduced a Bayesian probabilistic framework that allowed us to estimate  $p(R_i|S_{loc})$ , the probability that a plastic particle, sampled at the surface of the South Atlantic Ocean, came from a particular source. The framework supports different types of analyses and can be used, for example, to compute spatial probabilities, compute local probability as a function of particle age, or analyse the probabilities once a physical process (such as beaching) alters the particles' state.

The time average window used for computing the likelihood  $p(S_{loc}|R_i)$  can be adjusted according to the aim of the study. Usually, computing the likelihood for small time windows leads to greater variability in the likelihood and for instance in the posterior

270 probability. For these reasons, we computed the average likelihood on the whole simu-  
 271 lation and from there we computed the posterior probability.

272 As we showed in Figure 2, visualizing the posterior  $p(R_i|S_{loc})$  in maps allows us  
 273 to identify the most important sources that pollute ocean regions that provide high ecosys-  
 274 tem services and that are vulnerable to plastic, such as subtropical gyres (Helm, 2021)  
 275 and marine protected areas (Krüger et al., 2017). This can be used to prioritize the re-  
 276 duction of MPW in the principal sources to mitigate the problem. In particular, Porto  
 277 Alegre and Rio de Janeiro are the most probable sources of riverine plastic in the South  
 278 Atlantic Subtropical Gyre.

279 The local posterior age distributions, shown in Figure 3 further illustrate the anal-  
 280 ysis that can be done by selecting a location and by computing the probability distri-  
 281 butions as a function of the particle’s age. This can point us to the most likely source  
 282 if we estimate the time the plastic has been drifting in the ocean, by assessing its degra-  
 283 dation (Chamas et al., 2020; Gewert et al., 2015).

284 The latitudinal beached posterior probabilities, shown in Figure 4, demonstrate how  
 285 this framework can be used to analyse the contribution of different sources to particle  
 286 sinks (such as beaches) when considering certain physical processes that alter particle  
 287 pathways (such as the process of beaching). This can be expanded to including other ad-  
 288 ditional physical processes that can alter the dynamical state of the virtual particles, such  
 289 as sinking (Lobelle et al., 2021).

290 This study focuses on floating plastic coming from rivers that discharge plastic into  
 291 the South Atlantic. In our analysis, we ignore plastic entering the domain from the In-  
 292 dian Ocean leakage (Van der Mheen et al., 2019) and from the North Atlantic (Speich  
 293 et al., 2007). To consider it, we need to assume these leakages as sources, by knowing  
 294 how much plastic enters the domain through the boundaries, or expand the domain to  
 295 consider other basins.

296 One major advantage of the Bayesian nature of our framework is that it allows up-  
 297 dating the results when better estimates of plastic emissions are available without hav-  
 298 ing to redo the (computationally expensive) Lagrangian simulations. For instance, it can  
 299 be expanded by including a prior that accounts for seasonal variations in river-borne plas-  
 300 tic inputs, or by taking into account different types of land-based or sea-based sources.

### 301 Acknowledgments

302 This project was supported by NWO through grant OCENW.GROOT.2019.043. EvS  
 303 was partly supported through funding from the European Research Council (ERC) un-  
 304 der the European Union’s Horizon 2020 research and innovation programme (grant agree-  
 305 ment No 715386).

306 The output data from the simulations is available through [https://doi.org/10](https://doi.org/10.24416/UU01-90F027)  
 307 [.24416/UU01-90F027](https://doi.org/10.24416/UU01-90F027). The supporting figures, tables, and text can be found in the sup-  
 308 porting information file associated with this article.

### 309 References

- 310 Carlin, B. P., & Louis, T. A. (2008). *Bayesian methods for data analysis*. CRC  
 311 Press.
- 312 Chamas, A., Moon, H., Zheng, J., Qiu, Y., Tabassum, T., Jang, J. H., ... Suh, S.  
 313 (2020). Degradation rates of plastics in the environment. *ACS Sustainable*  
 314 *Chemistry & Engineering*, 8(9), 3494–3511.
- 315 Cózar, A., Echevarría, F., González-Gordillo, J. I., Irigoien, X., Úbeda, B.,  
 316 Hernández-León, S., ... others (2014). Plastic debris in the open ocean.

- 317 *Proceedings of the National Academy of Sciences*, 111(28), 10239–10244.
- 318 Davey, S., Gordon, N., Holland, I., Rutten, M., & Williams, J. (2016). *Bayesian*  
319 *methods in the search for mh370*. Springer Nature.
- 320 Delandmeter, P., & Sebille, E. v. (2019). The parcels v2. 0 lagrangian framework:  
321 new field interpolation schemes. *Geoscientific Model Development*, 12(8),  
322 3571–3584.
- 323 do Sul, J. A. I., & Costa, M. F. (2007). Marine debris review for latin america and  
324 the wider caribbean region: from the 1970s until now, and where do we go  
325 from here? *Marine Pollution Bulletin*, 54(8), 1087–1104.
- 326 Drillet, Y., Chune, S. L., Levier, B., & Drevillon, M. (2019). Smoc: a new global  
327 surface current product containing the effect of the ocean general circulation,  
328 waves and tides. In *Geophysical research abstracts* (Vol. 21).
- 329 Eriksen, M., Lebreton, L. C., Carson, H. S., Thiel, M., Moore, C. J., Borerro, J. C.,  
330 ... Reisser, J. (2014). Plastic pollution in the world’s oceans: more than 5  
331 trillion plastic pieces weighing over 250,000 tons afloat at sea. *PloS one*, 9(12),  
332 e111913.
- 333 Gewert, B., Plassmann, M. M., & MacLeod, M. (2015). Pathways for degradation  
334 of plastic polymers floating in the marine environment. *Environmental science:*  
335 *processes & impacts*, 17(9), 1513–1521.
- 336 Hardesty, B. D., Harari, J., Isobe, A., Lebreton, L., Maximenko, N., Potemra, J.,  
337 ... Wilcox, C. (2017). Using numerical model simulations to improve the  
338 understanding of micro-plastic distribution and pathways in the marine envi-  
339 ronment. *Frontiers in marine science*, 4, 30.
- 340 Helm, R. R. (2021). The mysterious ecosystem at the ocean’s surface. *PLoS Biology*,  
341 19(4), e3001046.
- 342 Jambeck, J., Hardesty, B. D., Brooks, A. L., Friend, T., Teleki, K., Fabres, J., ...  
343 others (2018). Challenges and emerging solutions to the land-based plastic  
344 waste issue in africa. *Marine Policy*, 96, 256–263.
- 345 Koelmans, B., Pahl, S., Backhaus, T., Bessa, F., van Calster, G., Contzen, N., ...  
346 others (2019). *A scientific perspective on microplastics in nature and society*.  
347 SAPEA.
- 348 Krüger, L., Ramos, J., Xavier, J., Grémillet, D., González-Solís, J., Kolbeinsson, Y.,  
349 ... others (2017). Identification of candidate pelagic marine protected areas  
350 through a seabird seasonal-, multispecific-and extinction risk-based approach.  
351 *Animal Conservation*, 20(5), 409–424.
- 352 Lacerda, A. L. d. F., Rodrigues, L. d. S., Van Sebille, E., Rodrigues, F. L., Ribeiro,  
353 L., Secchi, E. R., ... Proietti, M. C. (2019). Plastics in sea surface waters  
354 around the antarctic peninsula. *Scientific reports*, 9(1), 1–12.
- 355 Lebreton, L., & Andrady, A. (2019). Future scenarios of global plastic waste genera-  
356 tion and disposal. *Palgrave Communications*, 5(1), 1–11.
- 357 Lebreton, L., Slat, B., Ferrari, F., Sainte-Rose, B., Aitken, J., Marthouse, R., ...  
358 others (2018). Evidence that the great pacific garbage patch is rapidly accu-  
359 mulating plastic. *Scientific reports*, 8(1), 1–15.
- 360 Lobelle, D., Kooi, M., Koelmans, A. A., Laufkötter, C., Jongedijk, C. E., Kehl,  
361 C., & van Sebille, E. (2021). Global modeled sinking characteristics of  
362 biofouled microplastic. *Journal of Geophysical Research: Oceans*, 126(4),  
363 e2020JC017098.
- 364 Meijer, L. J., van Emmerik, T., van der Ent, R., Schmidt, C., & Lebreton, L. (2021).  
365 More than 1000 rivers account for 80% of global riverine plastic emissions into  
366 the ocean. *Science Advances*, 7(18), eaaz5803.
- 367 Morris, R. J. (1980). Plastic debris in the surface waters of the south atlantic. *Ma-*  
368 *rine Pollution Bulletin*, 11(6), 164–166.
- 369 Onink, V., Jongedijk, C., Hoffman, M., van Sebille, E., & Laufkötter, C. (2021).  
370 Global simulations of marine plastic transport show plastic trapping in coastal  
371 zones. *Environmental Research Letters*.

- 372 Onink, V., Wichmann, D., Delandmeter, P., & van Sebille, E. (2019). The role of  
373 Ekman currents, geostrophy, and Stokes drift in the accumulation of floating  
374 microplastic. *Journal of Geophysical Research: Oceans*, *124*(3), 1474–1490.
- 375 Richardson, H. R., Stone, L. D., et al. (1971). Operations analysis during the under-  
376 water search for scorpion. *Naval Research Logistics Quarterly*, *18*(2), 141–157.
- 377 Ryan, P. G. (2014). Litter survey detects the south Atlantic ‘garbage patch’. *Marine*  
378 *Pollution Bulletin*, *79*(1-2), 220–224.
- 379 Schofield, J., Wyles, K. J., Doherty, S., Donnelly, A., Jones, J., & Porter, A. (2020).  
380 Object narratives as a methodology for mitigating marine plastic pollution:  
381 multidisciplinary investigations in galápagos. *Antiquity*, *94*(373), 228–244.
- 382 Speich, S., Blanke, B., & Cai, W. (2007). Atlantic meridional overturning circulation  
383 and the southern hemisphere supergyre. *Geophysical Research Letters*, *34*(23).
- 384 Turner, A., Williams, T., & Pitchford, T. (2021). Transport, weathering and pol-  
385 lution of plastic from container losses at sea: Observations from a spillage of  
386 inkjet cartridges in the north Atlantic ocean. *Environmental Pollution*, *284*,  
387 117131.
- 388 Van der Mheen, M., Pattiaratchi, C., & van Sebille, E. (2019). Role of Indian Ocean  
389 dynamics on accumulation of buoyant debris. *Journal of Geophysical Research:*  
390 *Oceans*, *124*(4), 2571–2590.
- 391 Van Sebille, E., Aliani, S., Law, K. L., Maximenko, N., Alsina, J. M., Bagaev, A., ...  
392 others (2020). The physical oceanography of the transport of floating marine  
393 debris. *Environmental Research Letters*, *15*(2), 023003.
- 394 Van Sebille, E., Griffies, S. M., Abernathy, R., Adams, T. P., Berloff, P., Biastoch,  
395 A., ... others (2018). Lagrangian ocean analysis: Fundamentals and practices.  
396 *Ocean Modelling*, *121*, 49–75.
- 397 Van Sebille, E., Wilcox, C., Lebreton, L., Maximenko, N., Hardesty, B. D.,  
398 Van Franeker, J. A., ... Law, K. L. (2015). A global inventory of small  
399 floating plastic debris. *Environmental Research Letters*, *10*(12), 124006.